Silurian wildfire proxies and atmospheric oxygen

Glasspool, I.J., and Gastaldo, R.A.

Colby College, Waterville, ME 04901

Supplemental data

LOCALITIES AND AGE ASSIGNMENTS

Fossils were recovered from siltstone HF macerations of two localities: 1) The Rumney samples were collected from the Rumney Borehole drilled to a depth of 317.39 m by the British Geological Survey in 1978 (BGS ID: 382745/Ref: ST27NW618; 51°30'23.9", N 3°08'18.6"W) in the Cardiff-Cowbridge anticline near Rumney in South Wales. 2) The Winnica locality was collected by Mr. Andrzej Gorski in ~2013 from small outcrops either side of the Słupianka stream near Winnica in the Kielce region of Poland (N 50°52’24.5”, E 21°6’16.5”). The specimens come from the uppermost Słupianka Member of the Winnica Formation within the 5-7 m interval (see: Kozłowski 2003).

The Pen-y-lan Mudstone was deposited in an extensive marine setting that extended across the Midland Platform of the UK. Invertebrate-bearing siltstones of the formation indicate deposition in a shallow marine, mid-shelf setting, below normal wave base (Cherns et al., 2006). Both localities were deposited in the tropics to sub-tropics (Fig. 1). The Winnica Formation occurs in the Łysogóry Basin, which was bordered to the east by Baltica with islands to the southwest that are considered to be the source of the plant remains (Fig. 1; Bodzioch et al., 2003). Sediments were deposited under shallow to marginal marine conditions and grade laterally into continental mudstone and sandstone of the late Ludfordian Rachtanka Formation. The Słupianka Member is comprised of green fine-grained siliciclastics, marl, and argillaceous limestone, and represents a shallow nearshore environment. Plant remains include *Cooksonia*

(Bodzioch et al., 2003) and are most abundant in the middle sequences of bioturbated mudstone. They are associated with an estuarine fauna, comprised of lingulid brachiopods, ostracods, bivalves, and eurypterid fragments, preserved in a back-barrier to brackish setting.

The Pen-y-lan Mudstone is considered early Homerian and, based upon its shelly brachiopod fauna (Fry et al., 2017), is correlated with the Apedale Member of the Coalbrookdale Formation of the Welsh Borderland and South Wales. The presence of *Monograptus flemingii* in the lowermost beds of the formation at Pen-y-lan Quarry indicates a late Sheinwoodian to early Homerian (Ho1) age based on its correlation with the *Cyrtograptus rigidus* to *C. lundgreni* graptolite biozones at Builth Wells (Zalasiewicz and Williams, 1999). *Monograptus flemingii* is diachronous in its distribution, where it ranges from the Telychian *C. centrifugus* to *insectus* biozones in Arctic Canada (Zalasiewicz and Williams, 1999). Wojciech Kozłowski (pers comm. 2020) assigns an upper Ludfordian age to the Słupianka Member based upon chemostratigraphic correlation to the Lau Carbon Isotopic Excursion (CIE). The Lau CIE correlates with the *balticus-latilobus* graptolite Zone, considered equivalent to the lowermost part of the *Formosograptus formosus* Zone (Jeppsson et al., 2012).

OBSERVATIONS ON CHARACTERISTIC FEATURES OF CHARCOAL

When viewed by SEM, among the characteristic features of charcoal are: brittle fracture, high fidelity preservation of the original morphology, cell-wall homogenization, as well as other features including cuticular shrinkage, melting and blistering (see Edwards and Axe, 2004). Evaluated by reflected light microscopy, the reflectance of charcoal is typically elevated above that of non-charred material of comparable thermal rank maturation and features including brittle fracture and cell-wall homogenization may be observable. However, in Devonian to pre-

Devonian sediments charcoal is less often centimetre sized and blocky, a characteristic of charred woody vegetation, though some samples of *Prototaxites/Nematasketum* from localities such as the Lye Stream in the Welsh Borderlands of the UK do exhibit this morphology (Fig. S1). More frequently the charcoal morphology is constrained by the diminutive size of the plants or organs being charred. Similarly, cell-wall homogenization in charcoal was a feature first demonstrated in woody tissues with a lignin-rich middle lamellae, and which then became indistinguishable from the surrounding cellulose of the cell walls when charred at temperatures >300°C (Cope and Chaloner, 1980; Jones and Chaloner, 1991). However, subsequent research has shown this feature is not unique to lignified cell walls, as thermal (>350°C) cell-wall homogenization also has been demonstrated in fern sclerenchyma (McParland et al., 2007) and the bryophyte *Polytrichum* (Edwards and Axe, 2004). Outside of embryophytes, where discernible, we reviewed examples of permineralized *Prototaxites* in the literature (i.e. *P. loganii, P. southworthii* in Hueber, 2001; *Prototaxites* sp. in Graham et al., 2010; *P. taitii, P.* aff. *taitii* in Honegger et al., 2018). The cell walls of all examples of permineralized and uncharred *Prototaxites* were discrete and un-homogenized, where in contact with adjacent cells. This character was not commented upon by Scott and Glasspool (2007) in their observations on quantitative reflectance of charred *Ganoderma* (bracket fungus) used as a modern analogue. Review of the original images (Glasspool pers obs. 2022) indicates uncharred specimens with widely spaced hyphae, seldom touching. But, in those instances where they do, each of the hyphal walls remains discrete as in Hueber (2001, Plate 9). Anecdotally therefore, it appears that examples of *Prototaxites* and *Nematasketum* in the fossil record exhibiting cell wall homogenization, in association with a clean appearance and brittle fracture (cf. Edwards and Axe, 2004), were preserved by charring.

METHODS

Two 50 g subsamples of the Rumney Borehole core, one from each of the original driller sampling intervals at 314.71–316.3 m and 316.3-317.39 m, and 50 g of mudrock from one horizon at Winnica in the 5-7 m interval (see above), were disaggregated, and treated with hydrofluoric acid following standard protocols for mesofossil preparation. Previously published data collected by Glasspool on two localities, Ludford Lane (Glasspool et al., 2004) and North Brown Clee Hill (Glasspool et al., 2006) were used to construct Fig. 3. An additional new sample from North Brown Clee Hill was analyzed in 2022 and incorporated into the pre-existing data set. Additional data to support for Fig. 3 were gathered from further localities in the Welsh Borderlands (see below) but remain preliminary due to the restricted number of samples recovered. Macerated fossils were sieved to 150 microns. Phytoclasts (Gastaldo, 1994) were hand-picked under a dissecting microscope and prepared for both scanning electron microscope (SEM) analyses and subsequent reflectance microscopy.

Specimens for SEM analysis were first mounted on Pelco tabs, gold coated (approx. 90 seconds) using an SPI-Module sputter coater, and analysed with an Hitachi S-2700 scanning electron microscope. Where small size did not preclude practical preparation, a representative sample was selected for reflectance microscopy. This sub-sample was made to represent both the breadth of taxonomic diversity and differences in the apparent degree of charring (i.e., luster, color, fidelity of preservation). The selected specimens were removed from their tabs and set in silicon rubber square-tipped TEM moulds and embedded in a low viscosity epoxy resin (Struers Epofix) following ISO-7404-2, 1985 standards. Then, specimens were carefully oriented prior to resin hardening. Once hardened each individual block was re-embedded in Epofix in a larger mould for grinding and polishing.

In addition to the taxonomically significant material that followed this preparation pathway, a random selection of the remaining organic material was concentrated and embedded as a strew mount without prior electron microscopy and orientation. The aim of these strews was to provide an unbiased sampling of the material to explore the range of their physical properties in reflected light.

Epoxy blocks with the SEM and strew specimens were ground with a sequential series of abrasive papers, ranging from 120-5000 grit, before a penultimate polish on woven cloth dosed with 1 micron polycrystalline diamond suspension. Final polishing was done on a napped cloth with an 0.05 µm aluminium-oxide slurry.

Quantitative measurements (mean random reflectance in oil—R_o %) were made using a Leica DMR microscope fitted with a 50x oil immersion objective. Observations adhere to standard techniques (ISO-7404-5, 1994) though an Infinity 1 digital camera with Infinity Capture software was used for image acquisition. Calibration of the system and its linearity was conducted using at least four mineral standards closest in reflectance value to the material being measured. Standards used ranged from Spinel (R_o = 0.42%) to Silicon carbide (R_o = 7.93%). An oil blank was used, where necessary, to calibrate extremely low reflecting material. Where feasible, each specimen was measured at 100 points (1 point = 1 pixel, pixel size ~0.3 µm). However, the small scale of some specimens precluded meaningful counts of this size due to edge effects and imperfections of the polish, and as many points were counted as was practicable. The mean-random reflectances (R_o %) of samples were converted to temperatures using two equations: **Equation 1**) A composite 3^{rd} order polynomial trend-line from the experimental 1-24 hr duration charring data from Scott and Glasspool (2005: Table S1, Fig. S2), selected from a range of options as the most likely to yield the best results.

Scott and Glasspool (2005) 0.5 to 24 hr (combined), 3rd order polynomial calibration curve (Fig. S2) used to determine combustion temperature from reflectance

Equation 1: $y = 5.3103x^3 - 50.454x^2 + 206.87x + 220.17$

and, **Equation 2**) Data generated by Scott and Glasspool (2007: Table S2, Fig. S3) and in which modern *Ganoderma* (bracket fungus) was experimentally charred. This 3rd order polynomial trend-line was selected as a calibration curve, because it may better represent the original cell-wall chemistry of nematophytes and, in particular, *Prototaxites* with which bracket fungus has been compared (Boyce et al., 2007; see also Selosse, 2002**)**.

Scott and Glasspool (2007) 1 hr (*Ganoderma*), 3rd order polynomial calibration curve (Fig. S3) used to determine combustion temperature from reflectance

Equation 2: $y = 1.5242x^3 - 9.0073x^2 + 116.22x + 300.66$

To assess the impact of differing calibration data sets on estimated fire temperature, **Equations 1** and **2** are then compared with calibration data from Hudspith et al. (2014). These raw data, calibration curves, and comparisons are presented below (Tables S3-4, Figs. S4 to 5a-b).

Scott and Glasspool (2005) 1 hr, 3rd order polynomial calibration curve (Fig. S4) used to assess determine combustion temperature from reflectance

Equation 3: $y = 1.3269x^3 - 23.921x^2 + 167.53x + 234.31$

Scott and Glasspool (2005) 24 hr, 3rd order polynomial calibration curve (Fig. S4) used to assess determine combustion temperature from reflectance

Equation 4: $y = 5.659x^3 - 50.519x^2 + 194.92x + 208.55$

Hudspith et al. (2014; fig. 1) 1 hr, 3rd order polynomial calibration curve that may be used to determine the expected reflectance from a known charring temperature

Equation 5: $y = -6E\text{-}08x^3 + 0.0001x^2 - 0.044x + 5.9035$

Hudspith et al. (2014 [as measured by Glasspool]) 1 hr, 3rd order polynomial calibration curve that may be used to determine the expected reflectance from a known charring temperature

Equation 6: $y = -6E\text{-}08x^3 + 0.0001x^2 - 0.044x + 5.9061$

Hudspith et al. (2014 [as measured by Glasspool]) 1 hr, 3rd order polynomial calibration curve (**Equation 6)** data re-arranged. This permits the use of the Hudspith et al. (2014) experimental char data to assess preliminarily combustion temperature from reflectance

Equation 7: $y = 7.9525x^3 - 63.395x^2 + 229.08x + 262.82$

Equations 2, 3 are limited in their calibration precision beyond temperatures of 600°C and reflectances of R_o = 2.93% and 3.87%, respectively, the maxima of the raw calibration data.

In particular, the one-hour reflectance data from Scott and Glasspool (2007) begin to plateau as it reaches 600°C. The application of a 3rd order polynomial regression line to this data set, comparable to that applied by Hudspith et al. (2014), results in the data plateauing rapidly followed by a decline in reflectance values beyond R_o = ~5.5%. This contrasts with all the other regression lines presented that follow an exponential growth pattern. While the diminutive stature of the embryophytic vegetation and many of the nematophytes would only have supported combustion for very short durations, this curve does not provide a good model for higher reflectance values. Hence, it cannot be used exclusively. For the same reasons, the 24-hour charring duration data are unlikely to be applicable to the embryophytic vegetation. And, except for the differences in their basic chemistry, these data have more application to smoldering specimens of *Prototaxites*. The nematophytic elements of the vegetation are better represented by the Scott and Glasspool (2007) reflectance curve generated from charring *Ganoderma* for 1 hour at temperatures up to 600°C. While this curve can be applied to much of the higher reflectance nematophytic material, the curve falls outside of the calibration data set and is used with caution. The Hudspith et al. (2014) data were run with a shorter hold-duration of 1 hour and were extended to a higher temperature (800°C). However, we elect not to present the data from this curve that is based upon modern woods because the higher reflectance values it generates would yield improbably high fire temperatures; e.g., R_o 6.51% = temp. >1250°C. In view of the fact that the *Ganoderma* (**Equation 2**) and the Scott and Glasspool (2005) data (**Equations 1, 3-4**) were run on the same equipment, with the same parameters to maintain experimental consistency, we have elected use both the (**Equation 1 & 2**) calibrations, the latter being more applicable to some, possibly all, of the nematophytes.

A total of 67 phytoclasts were recovered from the Rumney Borehole from the two, short stratigraphic intervals at the base of the borehole (see above). These were analyzed by SEM, and 30 specimens (following the sub-sampling protocol above) were embedded for reflectance microscopy. An additional 40 specimens were analyzed from strew mounts (Table S5). Forty-four Winnica Fm. phytoclasts identified systematically were analyzed by SEM and, of these, where small size did not preclude practical preparation, a representative (in terms of taxonomic diversity and apparent degree of charring as observed in incident light) fourteen were selected for reflectance microscopy. An additional 72 phytoclasts were analyzed for reflectance from strew mounts. All specimens and data from the Rumney Borehole core are to be returned to the British Geological Survey, while all material and data from the Winnica locality are to be offered to the Smithsonian Institute as repository.

At Rumney, R_o % values range from 1.10–5.61%, greater than R_o % values from the Welsh Coalfield south of the Variscan orogenic front (Table S8). At their maximum, these are greater than the highest reflectance R_o = 3.29% reported by Bullock et al (2019) from the Cynheidre coalfield located along the Variscan Front. We note, though, that all these lithologic data (Table S8) originate from Carboniferous strata. At Winnica, vitrinitic phytoclasts measure R_o = 0.93%, lower than the (vitrinite reflectance equivalent) $R_{o\ eq}$ = 1.48/1.2% estimated by Schito et al. (2017) by converting $R_{o\ org}$ = 1.68% (the reflectance of organoclasts e.g., scolecodonts, graptolites and chitinozoans) using formulae in Xianming et al. (2000) and Petersen et al. (2013), respectively. If either the Rumney or Winnica R_o % values were the result of thermal maturation (rank), we would expect them to be constrained within a tight range. This does not accord with our data presented herein, and the reflectances of the mesofossils from both

Rumney and Winnica are more representative of a taphonomic history involving fire prior to burial (e.g., Jones and Chaloner, 1991; Scott and Glasspool, 2007; Glasspool and Scott, 2013).

Figure 3 Localities.

Descriptions of sampled beds or intervals for each locality identified in Fig. 3 from which charcoalified phytoclasts are suspected (i.e., published specimens that have the morphological characteristics of charcoal, but which have not been confirmed as such by direct observation by the authors) or documented, and used in the current analysis.

- ***Passage Creek***: Specimens come from horizons 8-9 in the lower Massanutten Sandstone along route 678 at the gap of Passage Creek, 6 km southeast of Strasburg, Virginia, USA (see Niklas and Smocovitis, 1983, fig. 20 & possibly figs. 22-25, now in the Paleobotanical Collections at Cornell as SEM stubs No. 1-16, and duplicate material). Tomescu et al. (2009) also describe material from Passage Creek and assign the locality to co-ordinates 38°56'43"N, 78°18'18"W. These authors assign the lower Massanutten Sandstone a Rhuddanian age, ca. 441 Ma.
    - While far from clear, fig. 20 in Niklas and Smocovitis (1983) illustrates a three-dimensionally preserved nematophytic mesofossil, composed of shard-like (i.e., brittle) elements similar to charred nematophytic fossils observed in this study by SEM and reflected light microscopy. Their figures 20, 22-25 also illustrate three-dimensionally preserved nematophytes, with evidence of internal anatomy (e.g., Niklas and Smocovitis, 1983, fig. 25 arrow) but without evidence of brittle fracture. As such, these specimens from high rank sediments in the Appalachians are suspected as being charred, but the original specimens have yet to be located at Cornell for study.
- ***Rumney Borehole***: Locality and age data are as detailed in the main paper.
- ***Lištice and Kosov Quarry***: Specimens come from the upper Wenlock (Homerian, *parvus-nassa* Biozone) of the Motol Member of the Liten Formation at the Lištice locality and

Kosov Quarry (spec. SILI-A1; see: Pšenička et al., 2021, fig. 6). Both localities are geographically near Beroun in the Barrandian area of the Prague Basin (Czech Republic). Specimens from these localities are stored in the West Bohemian Museum in Pilsen and the National Museum in Prague.

  - The fossils exhibit exquisite three dimensional anatomical preservation and clean brittle fracture (e.g., Pšenička et al., 2021, figs. 6c & 6f); further, these specimens were resistant to oxidative maceration in 65% HNO_3 for several minutes and up to 10 days (Pšenička et al., 2021). Such inert behavior to oxidative maceration is characteristic of charcoal. Graptolite and bitumen-reflectance data gathered from the Silurian of the western part of the Barrandian Basin indicate a regional thermal maturity of high to medium volatile bituminous rank for these samples (Suchý et al., 2002). The anatomical preservation, fracture style, and acid resistance indicate the probable preservation of this material as charcoal. However, it should be noted that the area is intruded by dykes and sills which cause elevated reflectance of organic particles that are immediately adjacent (within 3 m) of them. Suchý et al. (2002) note that regionally this effect is minor and given the preservation of the mesofossils seems an improbable element of their taphonomy.

- ***Port Clinton***: Specimens come from the Bloomsburg Formation in a road cut along state Route 61 at the northern corporate boundary of Port Clinton, Pennsylvania, USA. The specimens in fig. 8 of Strother (1988) are deposited at Harvard University Palaeobotanical Collection as specimens HUPC# 62280-62281. The locality is further discussed by Tomescu et al. (2009) who cite the co-ordinates of the location as 40°35'14"N, 76°01'34"W and assign it an Homerian–Gorstian age, ca. 423 Ma.

- Discussing the Bloomsburg Formation at Port Clinton and elsewhere in eastern Pennsylvania, Retallack (2015) reports a conodont color alteration index (CAI) of 4–4.5 and vitrinite reflectance of 3.5% in Silurian and Devonian rocks of the regions. He concludes that the sediments were buried to depths of 6.7–7.9 km and paleosols would have experienced compaction to 69% of their original volume. Figure 8 in Strother (1988) illustrates fragments of *Prototaxites* with high fidelity, three-dimensional anatomical preservation including uncrushed tubular elements with clean, brittle fractures. As above, these features, especially given their burial history, indicate preservation as charcoal.

- ***Nant Cwm Ddu*** a.k.a. *Nant y Cwm, Craig Cwm-du, Cwm Craig-Du, Cwm Graig Ddu* etc: The locality lies ~17 km SW of Builth Wells, Powys, south-central Wales. Samples were collected from the *Pterinea tenuistriata* Beds, *Wilsonia* Shales Formation in the Lower Ludlow Shales Group of Cwm Graig Ddu, in a small quarry on the west side of the road section (Grid Ref. SN 9622 4748 / 52°06′57″N, 003°31′01″W). The locality lies ~500 m south of the cattle grid, in the lower half of the *Pterinea* Beds just a few meters above the junction with the underlying ‘Shales with thin slumps’ division Gorstian stage ca. 420 Ma (Edwards et al., 1979; Edwards and Richardson, 2004; Edwards pers. comm. 2021).
  - Roberts et al. (1995) report a chitinozoan reflectance value of R_{ch} 2.31% for the *Lingula lata* Beds, part of the *Wilsonia* Shales (Straw, 1952), at Cwm Craig Ddu (SN 961 467). This equates to a low volatile bituminous to semi-anthracitic rank or a vitrinite reflectance between R_o = 1.5-2.0 % (see fig. 9 in Cole, 1994). Maceration of ~50 g of material from this study yielded material for analysis. Reflectance measurements undertaken as part of this study range from R_o = 2.12- 3.54%, $\bar{x}$ R_o = 2.58%, which is well above that reported by Roberts et al. (1995) for chitinozoans. In combination with features including

three dimensional anatomical preservation (Fig. S6), black silky luster, and brittle fracture, this fossil material is interpreted as charcoal.

- ***Wulff Land***: Samples described by Larsen et al. (1987) from Wulff Land, North Greenland, are estimated from Larsen et al. (1987, fig. 1) to have been collected at approx. 81°54'N, 50°44'W. The Nyeboe Formation occurs between the *Bohemograptus bohemicus*/*Saetograptus fritschi linearis* and *Pristiograptus dubius* biozones, indicating a Ludlow age.
    - Specimen GGU 319204 in Larsen et al. (1987, fig. 5) appears to be crowded with near centimeter sized, irregularly-shaped but blocky fragments. Some of these "coalified" specimens are tentatively assigned to *Prototaxites.* In describing their fig. 5, Larsen et al. (1987) compare the preservation with that of the Ludlow aged strata at Capel Horeb (see below). We would also draw comparison between their fig. 5 and hand specimens from the Lye Stream (Fig. S1) in which similar centimeter-sized blocky fragments are preserved. Glasspool also observes that, before charcoal became so widely studied in the literature, it was often mistakenly classified as "coalified" material and *vice-versa*. The Lye Stream material is definitively charcoal. The same conclusion cannot be drawn with any high degree of certainty about the Wulff Land material. But, the preservation is suggestive.
- ***Capel Horeb URCB***, (*Upper Roman Camp Beds Formation*) a.k.a. *Halfway Quarry:* Situated on the north side of the A40, 9 km east of Llandovery, Wales. Nat. Grid. Ref. SN83 8443 3234 (51°58′39″N, 003°41′02″W) the URCB are of lower Whitcliffian age. These beds are overlain unconformably by the lowermost Downtonian Long Quarry Beds (LQB). Plant fragments can be found throughout the URCB but are most abundant in grey blue siltstone layers near the top (Edwards and Rogerson, 1979).

- Maceration of ~50 g of material from the URCB by Glasspool yielded just nine mesofossils. But, of these, incident light microscopic examination indicates three appear to have characteristics of charring. More conclusively, SEM work by Edwards (1982) reveals three dimensional anatomically preserved mesofossils of prototaxodioid (e.g., Edwards, 1982, figs. 59-62 & 66-72) and nematothalloid types (e.g., Edwards, 1982, figs. 84-88) from this locality amid a greater number of compression fossils. These anatomically preserved fossils exhibit morphological and anatomical features closely comparable with the charred mesofossils from both Rumney and Winnica, and are considered, herein, to be charcoal.

- ***Winnica***: Locality and age data are as detailed in the main paper.
- ***Tin Mill Race***: Specimens come from Nat. Grid. Ref. SO45840 75208 (52°22′20″N, 002°47′49″W) in the Old Tin Mill Race (Fig. S7) alongside the River Teme near Downton Castle in Herefordshire, very close to the border with Shropshire, UK. Stratigraphically, the specimens come from the Přídolían, Temeside Shale, proximal to the Downton Bone Bed (Hauser, 2019).
  - In preparing fossils from Tin Mill Race, Lang (1937) reports that "The black pieces…were noticed to be harder and more promising for detailed investigation than many of the other carbonized specimens" and "owing to the opacity of the black material, had to be as thin as was practicable" (e.g., Lang, 1937, figs. 40-43). One of the characters of charred, as compared with coalified, fossils is that they are opaque in thin section (Jones and Rowe, 1999; Glasspool and Scott, 2013). Similarly, charcoal is also more rigid and fractures more during cutting and polishing. Maceration by Glasspool of ~50 g of material from Tin Mill Race, as with Capel Horeb, yielded mesofossils with characteristic features of charcoal.

- ***Ludford Lane***: Charred specimens from Nat. Grid. Ref. SO5116 7413 (52°21′47″N, 002°43′07″W), Ludford Lane, Ludlow, England (Glasspool et al., 2004) occur in the *Platyschima* Shale Member of the Downton Castle Formation and are assigned a Přídolían ~423 Ma age based upon their assignment to the *tripapillatus-spicula* sporomorph assemblage.
    - The occurrence of charcoal at this site has been established by Glasspool et al. (2004).
- ***Weir Quarry*** a.k.a. *Forge Rough Weir*: Charred specimens from Nat. Grid. Ref. SO4560 7525 (52°22′20″N, 002°48′01″W) occur on the opposite bank of the River Teme near Downton Castle, to Tin Mill Race (Fig. S7) in Herefordshire, UK. The age assignment is mid-Ludfordian, correlated with the rising arm of the Lau CIE ca. 424 Ma (Hauser, 2019). Maceration by Glasspool of ~50 g of material from Weir Quarry, as with Tin Mill Race and Capel Horeb, yielded mesofossils with characteristic features of charcoal.
- ***Perton Lane*:** Specimens come from Nat. Grid. Ref. SO 5943 3982 (52°03′19″N, 002°35′35″W) Perton Lane, near Hereford, England (see: Lang, 1937; Fanning, 1987; Fanning et al., 1988, 1990). The assemblage is within the Přídolí (?*ultimus*), lower *tripapillatus-spicula* sporomorph assemblage section of the Rushall beds.
    - Maceration by Glasspool of ~50 g of material from Perton Lane, as with the other Welsh borderland localities listed, yielded mesofossils with characteristic features of charcoal. Preliminary reflectance data from anatomically preserved material yields R_o = 1.31%. While low, this reflectance value indicates significantly greater thermal maturity than conodont alteration index data (CAI = 1.5 which approximates to an R_o <1.0%) from the Telychian, Upper Haugh Wood Beds of Woolhope, about 4 miles to the southeast (Bertram

et al., 1992). Condonts from Ludlow-aged deposits at Prior's Frome, ~1 mile to the southwest of Perton Lane, show no thermal alteration (Bertram et al., 1992).

- ***Capel Horeb LQB*** *(Long Quarry Beds Formation*) aka *Halfway Quarry:* Situated on the north side of the A40, 9 km east of Llandovery, Wales. Nat. Grid. Ref. SN8443 3234 (51°58′39″N, 003°41′02″W), the LQB are of lowermost Downtonian age (Edwards and Rogerson, 1979).
    - Maceration by Glasspool of a ~50 g of material from the Downtonian aged beds at Capel Horeb yielded a small number of mesofossils with characteristic features of charcoal.
- ***Podolia Borshchiv***: Specimens come from eleven sections in Podolia, southwestern Ukraine, in the escarpments of the Dniester River and its tributaries that include the Borschiv, Chortkiv, and Ivanye formations (See figs. 1-6 in Filipiak and Szaniawski, 2016). Samples from all formations are deposited at the Institute of Palaeobiology, Polish Academy of Science, Warsaw, Poland. The Borshchiv Formation is of lower to lower middle Lochkovian age.
    - The reasons for the interpretation of the mesofossils from the Lochkovian to Pragian of Podolia as charcoal are thoroughly, and convincingly, explored by Filipiak and Szaniawski (2016). Hence, these are not further discussed herein.
- ***Övedskloster***: The drillcore Övedskloster 2 comes from directly south of the Helvetesgraven sandstone quarry, c. 10 km NW of Sjöbo in Skåne, Sweden. As reported, the charcoal-bearing samples come from the Lochkovian of the Öved Sandstone (Mehlqvist et al., 2015).
    - Charcoal is specifically documented from this locality by Mehlqvist et al. (2015).

- ***Lye Stream***: Specimens come from outcrops along the Lye Stream near Morville, Shropshire, UK, Nat. Grid. Ref. SO67239290 (52°31′59″N, 002°29′04″W). These rocks are within the *uniformis* graptolite Biozone of the Lochkovian age Ditton Group (Ball and Dineley, 1961; Burgess and Edwards, 1991).
    - Specimens from this locality have the macro- (Fig. S1A), meso- and microscopic characteristics of charcoal viewed by incident and reflected light (Fig. S1B), and scanning electron microscopy.
- ***North Brown Clee Hill***: Specimens come from a stream section south of Monkhopton Church (Nat. Grid. Ref. SO62566 93406, 52°32′14″N, 002°33′12″W), North Brown Clee Hill, Shropshire, UK. The rocks are assigned to the Ditton Group within the Lochkovian, as determined biostratigraphically to be in the lower and middle sub zones of the *micronatus-newportensis* Biozone (see Ball and Dineley, 1961; Edwards et al., 1994).
    - Material from this locality is extensively documented as charred (Edwards and Axe, 2004; Glasspool et al., 2006; Morris et al., 2018).
- ***Podolia Chortkiv***: (See comments on the Podolia Borshchiv). The Chortkiv Formation is middle to upper Lochkovian.
- ***Podolia Ivanye***: (See comments on the Podolia Borshchiv). The Ivanye Formation is lower Pragian.
- ***Val d'Amour***: Samples come from the north side of Highway 11, about 200 m west of the intersection with Val d'Amour Road close to the Restigouche River in northern New Brunswick, Canada. The Val d'Amour Formation (Dalhousie Group) coaly shale comes from the Pragian-age Thompson Brook Member (Kennedy et al., 2013). *No inertinite/charcoal was recovered from the* ***Campbellton Formation*** *(as per Kennedy et al., 2013, table 1) and*

the text (also: Kennedy et al., 2012, p. 431), but not as recorded in fig. 7 the latter being incorrect. The inertinite from VA4 is considered to have been transposed into CF1 (pers. comm. Cortland Eble, 2021 who ran the maceral analysis). Therefore, the record in Lu et al., (2021) reporting Emsian charcoal in this Formation is in error.

  - Kennedy et al. (2013) report a variety of inertinitic macerals from the Val d'Amour, including fusinite. Although at very low concentrations, the occurrence of this maceral is strongly implies wildfire activity.

- ***Bad Münstereifel***: Carbonaceous shales (Brandschiefer) from Bad Münstereifel of the Rhenish Massif, Germany, contain inertinite (1.5% or 2.9% mineral matter free [mmf]; Wollenweber et al., 2006). These rocks are assigned an upper Lower Emsian age, from the Klerf-Formation (Stephan Schultka, Museum für Naturkunde Berlin pers. comm. 2021).
  - As above, the record of inertinite, though at very low concentrations, indicates wildfire activity.

Comments on Localities in Lu et al. (2021)

In a recent examination of wildfire/charcoal, Lu et al. (2021) list fourteen Silurian to Early Devonian localities (Lu et al., 2021, supplemental tables S2A and S2B). Lu et al. (2021) exclude one report of charcoal, that of Pflug & Prössl (1989, 1991) from the 'Pragian' of Germany (table S2B), but do not indicate why. We concur with this exclusion because the authors (Pflug & Prössl, 1989) do not temporally constrain the fusinite they document beyond indicating a Lower Devonian age, which is too vague to be of chronostratigraphic use. Further, the fusinite occurs in sillimanitic gneiss indicating metamorphic temperatures in excess of 600°C, more than sufficient to alter tracheids to fusinite. As such, metamorphism cannot be excluded as the taphonomic mechanism of formation for these (as illustrated) <50 µm sized fusinite fragments.

Of the 13 localities included by Lu et al. (2021), we would note that their age assignment for the Pen-y-lan Mudstone as Lochkovian, Ditton is incorrect, as well as the depositional environment, reported as terrestrial (see main text). It is possible that they are referring to the Lye Stream locality (discussed above), on which Burgess and Edwards (1988) base their type material for *Nematasketum diversiforme*. However, there is no explicit reference to this locality in Lu et al. (2021). It is possible that the locality could be their "D1: Lochkovian; FC-Fossil; Eura: Avalonia (26°S); (Shropshire); Ditton; SLT; terrestrial Burgess & Edwards 1988" locality", although that could equally well be referring to Targrove Quarry (Burgess and Edwards, 1988). Confusingly, the fossils from neither Targrove nor Lye Stream were collected from siltstones, but from "a coarse sandstone with reworked cornstones".

The evidence of wildfire from the southern Tunisia, Lochkovian age, Tadrart Formation of the Ghadamis Basin comprises the polycyclic aromatic hydrocarbons (PAHs) pyrene, fluoranthene, and benzo[a]anthracene (Romero-Sarmiento et al. 2011). Benzo[a]anthracene has been reported elsewhere from Cambrian and lower Ordovician aged rocks (Li et al., 2012), and these are unlikely to be of wildfire origin. The potential non-wildfire derived sources of PAHs are discussed extensively in Belcher et al. (2005). But; it is perhaps noteworthy that pyrene, fluoranthene, and benzo[a]anthracene may be associated with petrogenic inputs (Huang et al., 2015). This is a potential source of these PAHs in the Tadrart Formation given demonstrated migration conduits from the Tanezzuft Formation (Underdown and Redfern, 2008). In short, the presence of PAHs without other corroborating evidence cannot be viewed as conclusive proof of fires.

The omission of the Campbellton Formation from our list of early Devonian localities was discussed above with the Val d'Amour material. Also, as presented above, we observe that the Bad Münstereifel locality is of upper lower Emsian age and not Pragian.

As part of a much broader Phanerozoic-wide assessment of inertinite occurrences and atmospheric oxygen concentration, a maceral count was made of the L'Anse-á-Brillant coal seam at Tar Point on the Gaspé Peninsula, Canada (Glasspool and Scott, 2010). This demonstrated the coal to be dominated by vitrinite and liptinite, but with the lowest possible percentage of inertinite (macrinite = 0.2%, [0.3% mmf] based upon a 500 point count). This data point, along with the Val d'Amour inertinite (Kennedy et al., 2013) whether included or excluded from the two analyses (Glasspool and Scott, 2010; Glasspool et al., 2015), had negligible impact on the interpretation of atmospheric oxygen concentration in the 10 or 15 million year binning intervals within which they fell (see: Glasspool et al., 2015). While this single fragment of macrinite may permit L'Anse-á-Brillant to be very tentatively scored as evidence of wildfire activity, it should not be done so without qualification or given undue weighting. The occurrence of wildfire at Val d'Amour is slightly more convincing. Of the four beds/blocks sampled here, the inertinite concentration ranged from 0 to 2.0% mmf (x = 0.8% mmf). However, most of this inertinite was classifiable as either fusinite or semifusinite (x = 0.5% mmf), both of which are strongly associated with a wildfire related taphonomy (Glasspool and Scott, 2013). This was more pronounced in one sample where of the 2.0% mmf inertinite, over half was fusinite. Therefore, we have elected to show Val d'Amour in Fig. 3 and not L'Anse-á-Brillant as evidence of fire.

Tables

Table S1 (Excel file). Experimental charring data gathered by Scott and Glasspool (2005). Specimens were charred at durations ranging from 0.5 to 24 hrs and temperatures from 200 to 900°C, from which the resulting mean random reflectance (R_o %) for each charring run was determined.

Table S2 (Excel file). Experimental charring data gathered by Scott and Glasspool (2007). Specimens of the bracket fungus (*Ganoderma*) were charred for 1 hour at temperatures between 300 and 600°C and the resulting mean random reflectance (R_o %) for each charring run determined.

Table S3 (Excel file). Hudspith et al. (2014) 1 hr hold-duration experimental charring calibration data. *Hudspith et al. (2014) only presented the raw data in chart format. However, the calibration equation as presented could not be used to calculate temperature of formation from mean random reflectance. To permit these data to be used for the calculation of temperature, Glasspool precisely measured the points and replotted them in Excel (herein shown as measured).*

Table S4 (Excel file). Application of calibration equations to nominal reflectance values (R_o = 0.25-6.5%) to permit an assessment of their impact on temperature estimates. *Within the column headers, Max = the maximum experimental charring temperature used for each run, and R_o % the maximum mean random reflectance measured. Data in* ***bold*** *correspond to values beyond the calibration ranges.*

Table S5 (Excel file). List of Rumney, Winnica, Ludford Lane, and North Brown Clee Hill specimen morphotypes, their associated mean random reflectance (Ro %), recorded as an average of 100 data points (measured as pixels). Where less than 100 points were sampled, the number measured (n =) is given next to the Id#. (Temp. w°C) is the fire temperature calculated from the Ro % using **Equation 1** based upon modern woods. (Temp. g°C) is the fire temperature calculated from the Ro % using **Equation 2** based upon the modern bracket fungus *Ganoderma*. Mean, min, and max Temp. °C data are summarized in Table S6.

Notes on Table S5:

1) UP = Unclassified phytoclast. A phytoclast of embryophytic or nematophytic origin, but with insufficient preservation to permit a robust taxonomic assignment. Such phytoclasts are typically either extremely compressed, gelified/vitrinised, or highly fragmented, but often preserve some very limited area of relic cellular structure. This relic structure may suggest affinity to a certain morphogroup, but is not sufficiently distinct to permit systematic classification with confidence. Most of the UPs are strew mount specimens and, as such, are viewed as a single randomly oriented 2-dimensional polished section through a much larger 3-dimensional clast. Organic petrographic nomenclature deals exclusively with particles viewed in reflected light and terms such as “Vitrinite” and “Inertinite”, as currently defined by the ICCP; do not translate well to cross-disciplinary studies due to the taxonomic and morphologic constraints the petrographic definitions entail.

2) W.Strew-23 and W.Strew-22 are duplicated in Table S5 as these clasts preserve both vitrinitic and inertinitic elements.

3) Based upon its comparatively advanced morphology and low reflectance (R_o = 0.4%), W.SEM-3 was dropped from the analysis as suspected post-Silurian contaminant.

Table S6 (Excel file). Summary of the mean, minimum, and maximum charring temperatures (°C) calculated from the Winnica and Rumney Borehole data in Table S5. The two sets of summary data (w and g) represent the application of **Equation 1** based upon modern woods and **Equation 2** based upon the modern bracket fungus *Ganoderma*.

Table S7 (Excel file). Reflectance (R_o %) data measured in 2022 from an additional prototaxodioid specimen from North Brown Clee Hill. The calibration curve for conversion from raw grey scale values to R_o % is given. These data are incorporated with those from Glasspool et al. (2006) into Table S5.

Table S8 (Excel file). Regional rank maturation data from Bullock et al., (2019).

Figures

Fig. S1. *Prototaxites* from Lye Stream. a) Roughly centimeter sized charred fragments in hand specimen (scale: each division = 1 mm). b) Polished section viewed at 20x magnification showing a roughly transverse cut through the large tubes, though several are in longitudinal section. Preliminary quantitative measurement of this specimen indicates a maximum R_o = 5.68%.

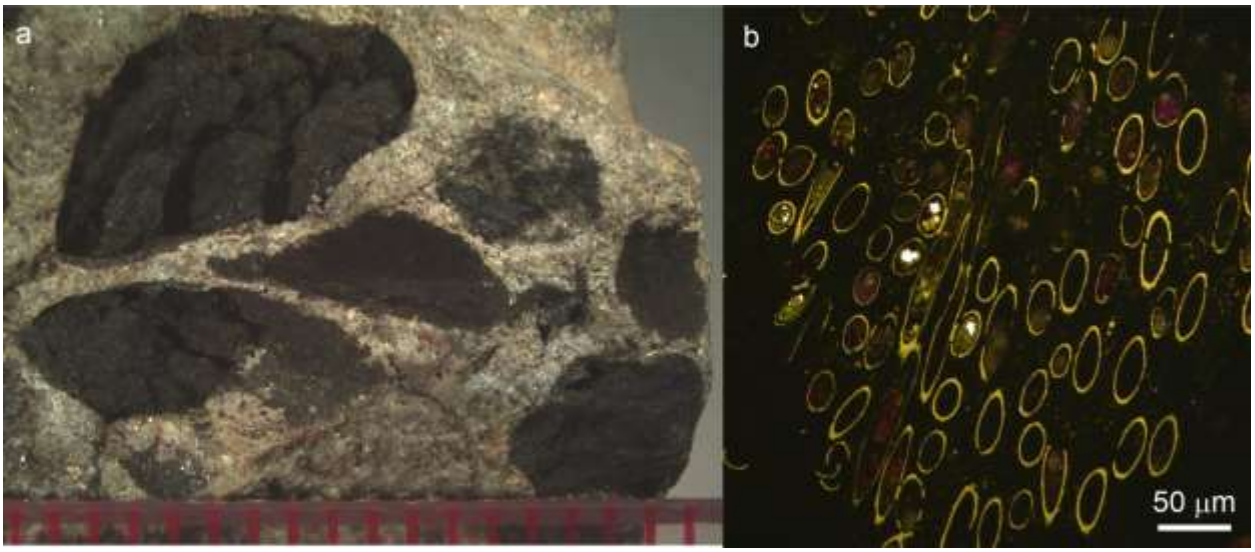

Figure S2. 0.5 to 24hr (composite) 3rd order polynomial calibration curve (**Equation 1**) plotted from the experimentally charred wood data in **Table S1** (Excel file).

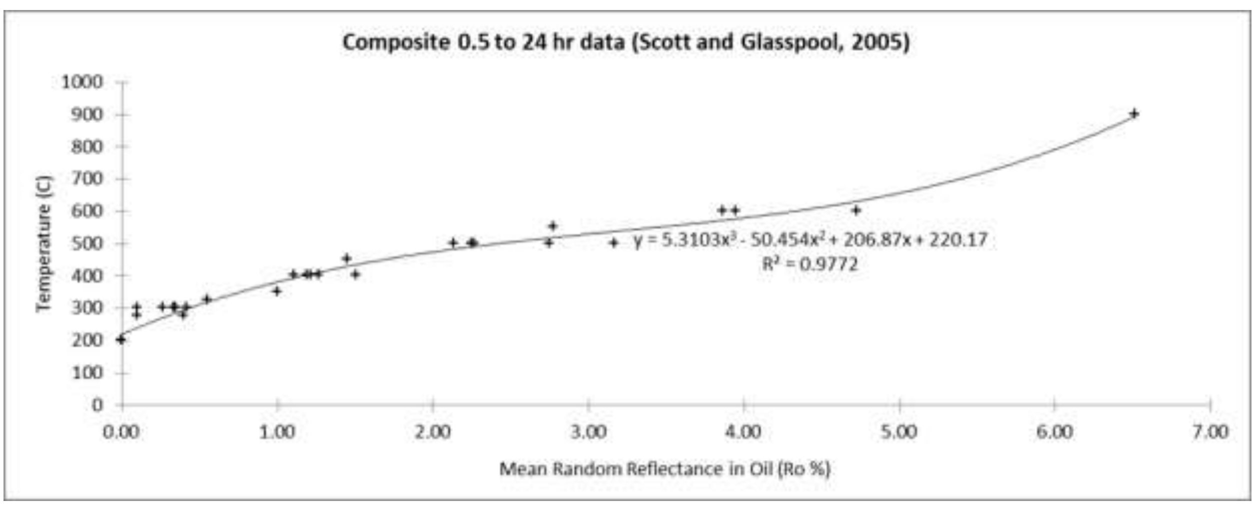

Figure S3. 3rd order polynomial calibration curve (**Equation 2**) plotted for *Ganoderma* charred for 1 hour. Data in **Table S2** (Excel file).

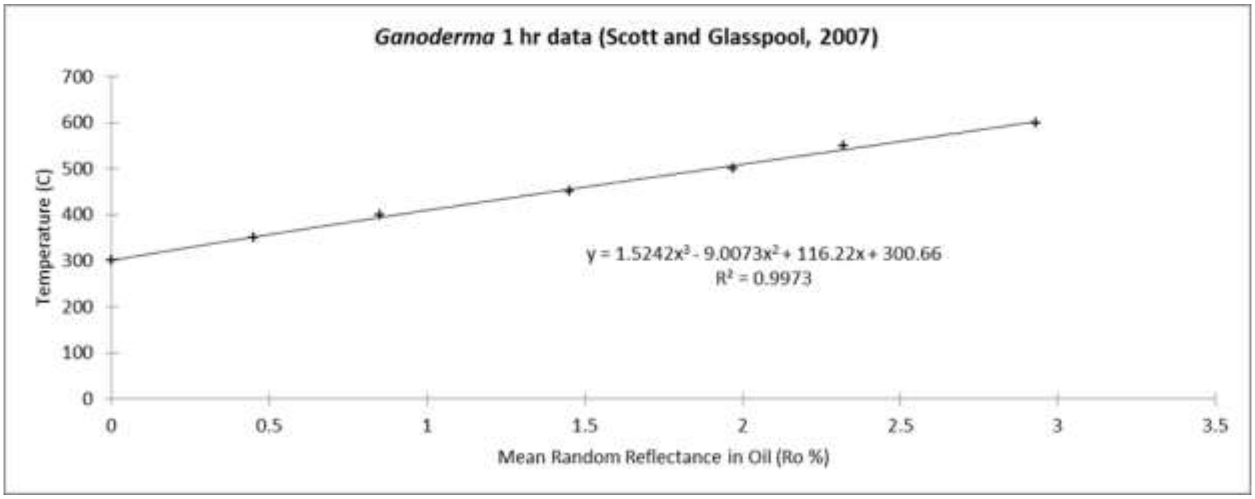

Figure S4. 1 hr (**Equation 3**) and 24 hr (**Equation 4**) 3rd order polynomial calibration curves plotted from charred wood data in **Table S1** (Excel file).

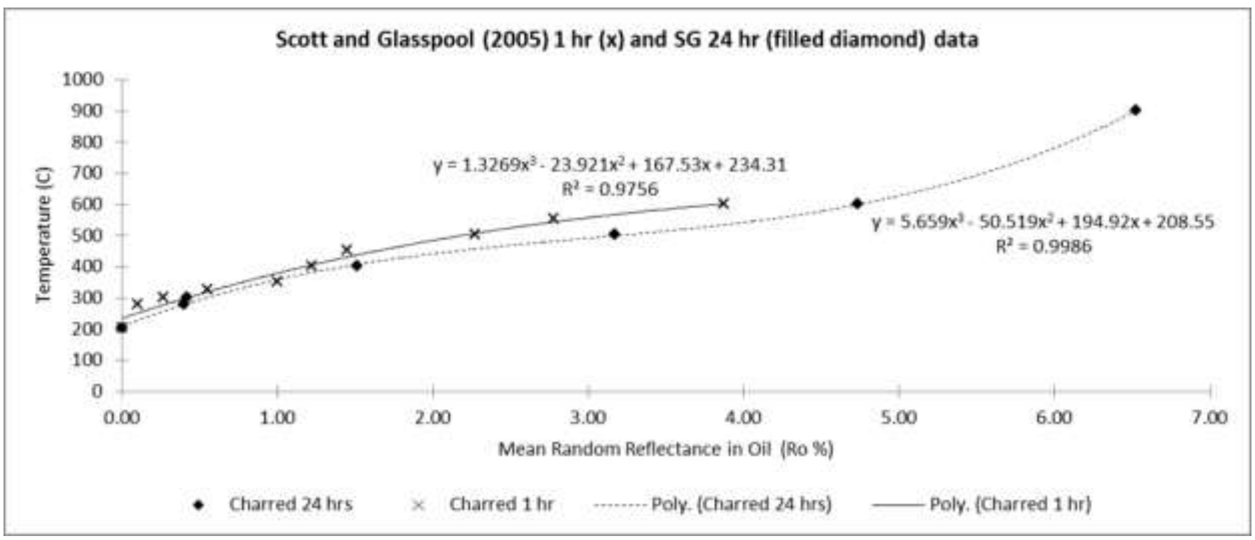

Figure S5a. Hudspith et al. (2014) 1 hr hold-duration experimental charring calibration data as measured by Glasspool (**Equation 6**). Data in **Table S3** (Excel file). *We note that the original equation in Hudspith et al. (2014) and that produced by Glasspool's measurements differ very slightly (**bold**).*

Original Hudspith et al. (2014: their Fig. 1) 3rd order polynomial calibration

Equation 5: *$y = -6E\text{-}08x^3 + 0.0001x^2 - 0.044x + 5.90\underline{\mathbf{35}}$*

Glasspool measured 3rd order polynomial calibration (Fig. S5a)

Equation 6*: $y = -6E\text{-}08x^3 + 0.0001x^2 - 0.044x + 5.90\underline{\mathbf{61}}$*

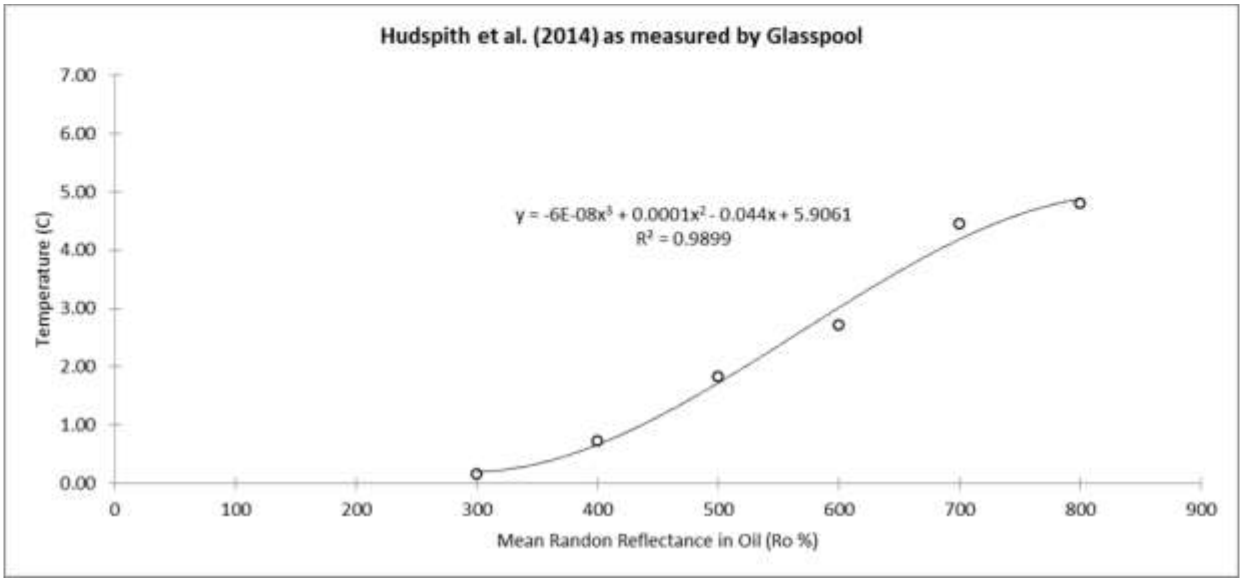

Figure S5b. Fig. S5a / **Equation 6** re-arranged with the axes inverted to allow calculation of temperature from reflectance.

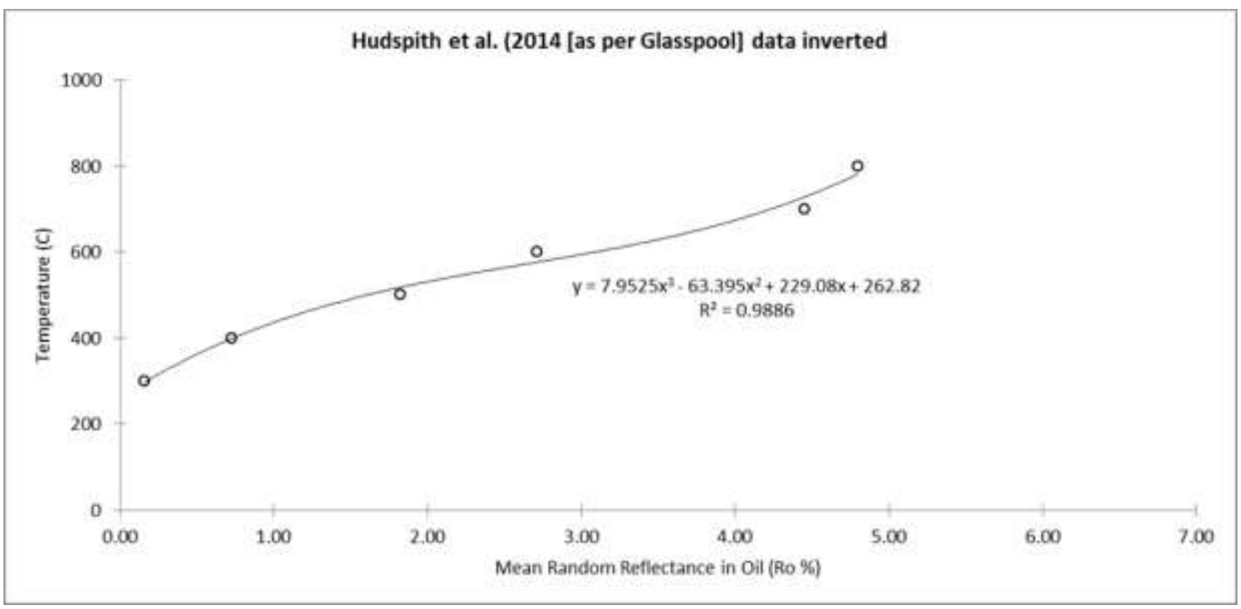

Fig. S6 Prototaxodioid from Nant Cwm Ddu viewed in reflected light x50. LT = large tubes, here with open, uncompressed lumens and walls exhibiting brittle fracture. FT = fine tube ground mass, largely destroyed, in part by the growth of pyrite (Py).

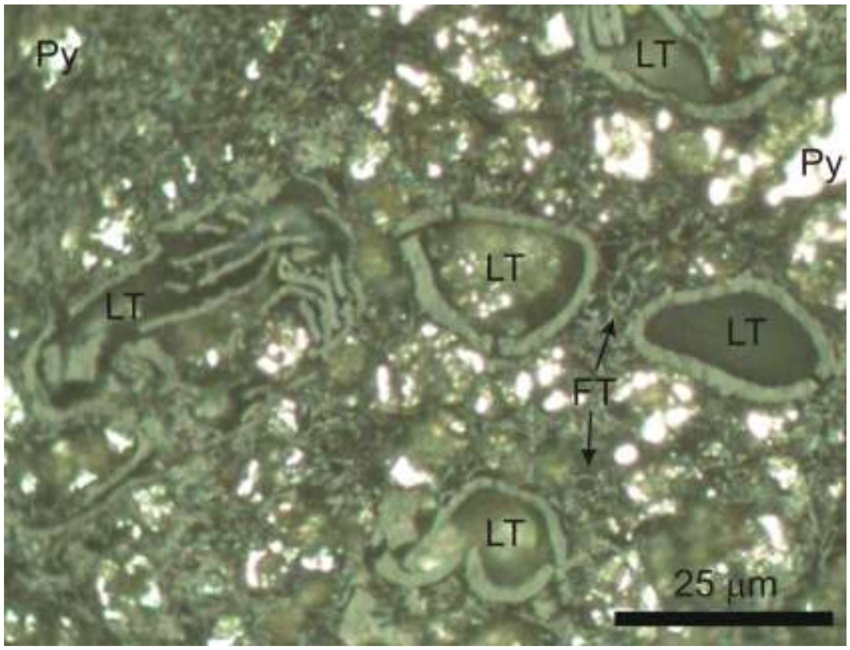

Fig. S7. Tin Mill Race locality near Downton Castle, Herefordshire.

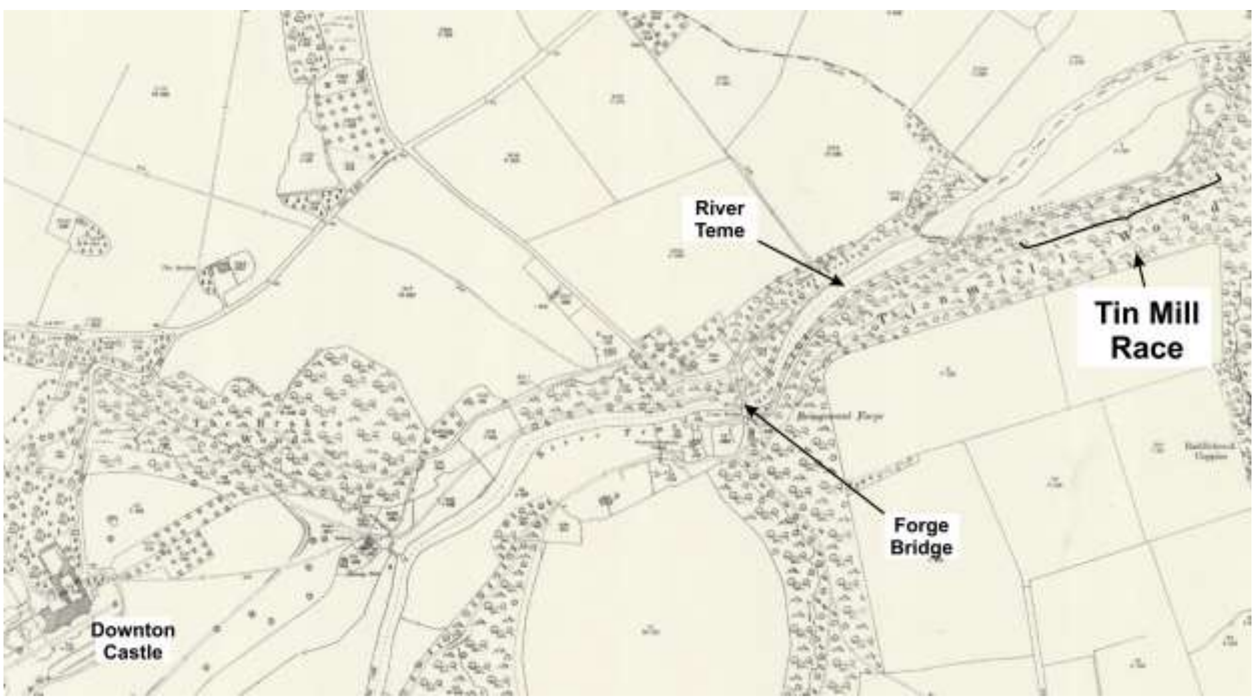

Citations

Ball, H.W. and Dineley, D.L., 1961, The Old Red Sandstone of Brown Clee Hill and the adjacent area: I Stratigraphy: British Museum (Natural History) Geology, v. 5 p. 175-242.

Belcher, C.M., Collinson, M.E. and Scott, A.C., 2005, Constraints on the thermal energy released from the Chicxulub impactor: new evidence from multi-method charcoal analysis: Journal of the Geological Society, v. 162, no. 4, p. 591-602.

Bertram, C.J., Elderfield, H., Aldridge, R.J. and Morris, S.C., 1992, $^{87}Sr/^{86}Sr$, $^{143}Nd/^{144}Nd$ and REEs in Silurian phosphatic fossils: Earth and Planetary Science Letters, v. 113, no., 1-2, p. 239-249.

Bodzioch, A., Kozłowski, W. and Poplawska, A., 2003, A *Cooksonia*-type flora from the Upper Silurian of the Holy Cross Mountains, Poland: Acta Palaeontologica Polonica, v. 48, no. 4, p. 653-656.

Boyce, C.K., Hotton, C.L., Fogel, M.L., Cody, G.D., Hazen, R.M., Knoll, A.H. and Hueber, F.M., 2007, Devonian landscape heterogeneity recorded by a giant fungus: Geology, v. 35, no. 5, p. 399-402.

Burgess, N.D. and Edwards, D., 1988, A new Palaeozoic plant closely allied to *Prototaxites* Dawson: Botanical Journal of the Linnean Society, v. 97, no. 2, p. 189-203.

Burgess, N.D. and Edwards, D., 1991, Classification of uppermost Ordovician to Lower Devonian tubular and filamentous macerals from the Anglo-Welsh Basin: Botanical Journal of the Linnean Society, v. 106, p. 41-66.

Bullock, L., Parnell, J., Muirhead, D., Armstrong, J., Schito, A. and Corrado, S., 2019, A thermal maturity map based on vitrinite reflectance of British coals: Journal of the Geological Society, v. 176, p. 1136-1142. https://doi.org/10.1144/jgs2019-055

Cherns, L., Cocks, L.R.M., Davies, J.R., Hillier, R.D., Waters, R.A. and Williams, M., 2006, Silurian: the influence of extensional tectonics and sea-level changes on sedimentation in the Welsh Basin and on the Midland Platform: *in* Brenchley, P.J., and Rawson, P.F. eds., The geology of England and Wales, second edition. Geological Society of London, p. 75-102. https://doi.org/10.1144/GOEWP.

Cole, G.A., 1994, Graptolite-chitinozoan reflectance and its relationship to other geochemical maturity indicators in the Silurian Qusaiba Shale, Saudi Arabia: Energy & Fuels, v. 8, no. 6, p. 1443-1459.

Cope, M.J. and Chaloner, W.G., 1980, Fossil charcoal as evidence of past atmospheric composition: Nature, v. 283, no. 5748, p. 647-649.

Edwards, D., 1982, Fragmentary non-vascular plant microfossils from the late Silurian of Wales: Botanical Journal of the Linnean Society, v. 84, no. 3, p. 223-256.

Edwards, D. and Axe, L., 2004, Anatomical evidence in the detection of the earliest wildfires: Palaios, v. 19, no. 2, p. 113-128.

Edwards, D. and Richardson, J.B., 2004, Silurian and Lower Devonian plant assemblages from the Anglo-Welsh Basin: a palaeobotanical and palynological synthesis: Geological Journal, v. 39, p. 375-402.

Edwards, D. and Rogerson, E.C.W., 1979, New records of fertile Rhyniophytina from the late Silurian of Wales: Geological Magazine, v. 116, p. 93-98.

Edwards, D., Bassett, M.G. and Rogerson, E.C.W., 1979, The earliest vascular land plants: continuing the search for proof: Lethaia, v. 12, p. 313-324.

Edwards, D., Fanning, U. and Richardson, J.B., 1994, Lower Devonian coalified sporangia from Shropshire: *Salopella* Edwards & Richardson and *Tortilicaulis* Edwards: Botanical Journal of the Linnean Society, v. 116, p. 89-110.

Fanning, U., 1987, Late Silurian-Early Devonian plant assemblages in the Welsh borderland: (Doctoral dissertation, University College).

Fanning, U., Richardson, J.B. and Edwards, D., 1988, Cryptic evolution in an early land plant: Evolutionary Trends in Plants (ETP), v. 2, no. 1, p. 13-24.

Fanning, U., Edwards, D. and Richardson, J.B., 1990, Further evidence for diversity in late Silurian land vegetation: Journal of the Geological Society, v. 147, no. 4, p. 725-728.

Filipiak, P., and Szaniawski, H., 2016, Nematophytes from the Lower Devonian of Podolia, Ukraine: Review of Palaeobotany and Palynology, v. 224, p. 109-120. doi:10.1016/j.revpalbo.2015.09.005

Fry, C.R., Ray, D.C., Wheeley, J.R., Boomer, I., Jarochowska, E., and Loydell, D.K., 2017, The Homerian carbon isotope excursion (Silurian) within graptolitic successions on the Midland Platform (Avalonia), UK: implications for regional and global comparisons and correlations: GFF, v. 139, p. 301–31.

Gastaldo, R.A., 1994, The genesis and sedimentation of phytoclasts with examples from coastal environments: *in* Traverse, A., ed., Sedimentation of Organic Particles. Cambridge University Press, p. 103-127.

Glasspool, I.J. and Scott, A.C., 2010, Phanerozoic concentrations of atmospheric oxygen reconstructed from sedimentary charcoal: Nature Geoscience, v. 3, no. 9, p. 627-630.

Glasspool, I.J. and Scott, A.C., 2013, Identifying past fire events *in* Belcher, C.M. ed., Fire phenomena and the Earth system: an interdisciplinary guide to fire science: John Wiley & Sons, Ltd. p. 229–229.

Glasspool I.J., Edwards, D., and Axe, L., 2004, Charcoal in the Silurian as evidence for the earliest wildfire: Geology, v. 32, p. 381–383. https://doi.org/10.1130/G20363.1

Glasspool, I.J., Edwards, D. and Axe, L., 2006, Charcoal in the Early Devonian: a wildfire-derived Konservat–Lagerstätte: Review of Palaeobotany and Palynology, v. 142, no. 3-4, p. 131-136.

Glasspool, I.J., Scott, A.C., Waltham, D., Pronina, N.V. and Shao, L., 2015, The impact of fire on the Late Paleozoic Earth system: Frontiers in Plant Science, v. 6, p. 756.

Graham, L.E., Cook, M.E., Hanson, D.T., Pigg, K.B. and Graham, J.M., 2010, Structural, physiological, and stable carbon isotopic evidence that the enigmatic Paleozoic fossil *Prototaxites* formed from rolled liverwort mats: American Journal of Botany, v. 97, no. 2, p. 268-275.

Hauser, L.M., 2019. The upper Silurian Downton Bone Bed of Weir Quarry, Herefordshire, England: (Doctoral dissertation, University of Portsmouth).

Honegger, R., Edwards, D., Axe, L. and Strullu-Derrien, C., 2018, Fertile *Prototaxites taiti*: a basal ascomycete with inoperculate, polysporous asci lacking croziers: Philosophical Transactions of the Royal Society B: Biological Sciences, v. 373, no. 1739, p. 20170146.

Huang, H., Zhang, S. and Su, J., 2015, Pyrolytically derived polycyclic aromatic hydrocarbons in marine oils from the Tarim Basin, NW China: Energy & Fuels, v. 29, no. 9, p. 5578-5586.

Hudspith, V.A., Belcher, C.M. and Yearsley, J.M., 2014, Charring temperatures are driven by the fuel types burned in a peatland wildfire: Frontiers in Plant Science, v. 5, p. 714.

Hueber, F.M., 2001, Rotted wood–alga–fungus: the history and life of *Prototaxites* Dawson 1859: Review of Palaeobotany and Palynology, v. 116, no. 1-2, p. 123-158.

ISO-7404-2:1985, 1985, Methods for the petrographic analysis of bituminous coal and anthracite: Part 2: Method of preparing coal samples: Geneva, International Organization for Standardization, 8 p.

ISO 7404-5: 1994, 1994, Methods for the petrographic analysis of bituminous coal and anthracite-part 5; methods of determining microscopically the reflectance of vitrinite: Geneva, International Organization for Standardization, 12 p.

Jeppsson, L., Talent, J.A., Mawson, R., Andrew, A., Corradini, C., Simpson, A.J., Wigforss-Lange, J. and Schönlaub, H.P., 2012, Late Ludfordian correlations and the Lau event: *in* Talent, J.A., ed., Earth and Life: Global Biodiversity, Extinction Intervals and Biogeographic Perturbations Through Time. Springer, Dordrecht, p. 653-675.

Jones, T.P. and Chaloner, W.G., 1991, Fossil charcoal, its recognition and palaeoatmospheric significance: Palaeogeography, Palaeoclimatology, Palaeoecology, v. 97, no. 1-2, p. 39-50.

Jones, T.P., and Rowe, N.P., 1999, Plant cell walls. *in*: Jones, T.P., and Rowe, N.P., eds., Fossil plants and spores: modern techniques: Geological Society, London, p. 116-120.

Kennedy, K.L., Gensel, P.G. and Gibling, M.R., 2012, Paleoenvironmental inferences from the classic Lower Devonian plant-bearing locality of the Campbellton Formation, New Brunswick, Canada: Palaios, v. 27, no. 6, p. 424-438.

Kennedy, K.L., Gibling, M.R., Eble, C.F., Gastaldo, R.A., Gensel, P.G., Werner-Zwanziger, U. and Wilson, R.A., 2013, Lower Devonian coaly shales of northern New Brunswick, Canada: plant accumulations in the early stages of terrestrial colonization: Journal of Sedimentary Research, v. 83, p. 1202-1215.

Kozłowski, W., 2003, Age, sedimentary environment and palaeogeographical position of the Late Silurian oolitic beds in the Holy Cross Mountains (Central Poland): Acta Geologica Polonica, v. 53, no. 4, p. 341-357.

Lang, W.H., 1937, On the plant-remains from the Downtonian of England and Wales: Philosophical Transactions of the Royal Society of London. Series B, Biological Sciences, v. 227, no. 544, p. 245-291.

Larsen, P.H., Edwards, D. and Escher, J.C., 1987, Late Silurian plant megafossils from the Peary Land Group, North Greenland: Rapport Grønlands Geologiske Undersøgelse, v. 133, p. 107-112.

Li, M., Shi, S. and Wang, T.G., 2012, Identification and distribution of chrysene, methylchrysenes and their isomers in crude oils and rock extracts: Organic Geochemistry, v. 52, p. 55-66.

Lu, M., Ikejiri, T. and Lu, Y., 2021, A synthesis of the Devonian wildfire record: Implications for paleogeography, fossil flora, and paleoclimate: Palaeogeography, Palaeoclimatology, Palaeoecology, v. 571, p. 110321. https://doi.org/10.1016/j.palaeo.2021.110321.

McParland, L.C., Collinson, M.E., Scott, A.C., Steart, D.C., Grassineau, N.V. and Gibbons, S.J., 2007, Ferns and fires: experimental charring of ferns compared to wood and implications for paleobiology, paleoecology, coal petrology, and isotope geochemistry: Palaios, v. 22, no. 5, p. 528-538.

Mehlqvist, K., Steemans, P. and Vajda, V., 2015, First evidence of Devonian strata in Sweden—A palynological investigation of Övedskloster drillcores 1 and 2, Skåne, Sweden: Review of Palaeobotany and Palynology, v. 221, p. 144-159.

Morris J.L., Edwards D., and Richardson, J.B., 2018, The advantages and frustrations of a plant Lagerstätte as illustrated by a new taxon from the Lower Devonian of the Welsh Borderland, UK. *in*: Krings, M., Harper, C.J., Cuneo, N.R., Rothwell, G.W., eds., Transformative Paleobotany: papers to commemorate the life and legacy of Thomas N Taylor. London, UK: Academic Press, p. 49–67.

Niklas, K.J. and Smocovitis, V., 1983, Evidence for a conducting strand in early Silurian (Llandoverian) plants: implications for the evolution of the land plants: Paleobiology, v. 9, p. 126-137.

Petersen, H.I., Schovsbo, N.H. and Nielsen, A.T., 2013, Reflectance measurements of zooclasts and solid bitumen in Lower Paleozoic shales, southern Scandinavia: Correlation to vitrinite reflectance: International Journal of Coal Geology, v. 114, p. 1-18. https://doi.org/10.1016/j.coal.2013.03.013

Pflug, H.D. and Prössl, K.F., 1989, Palynology in gneiss-Results from the continental deep drilling program: Naturwissenschaften, v. 76, no. 12, p. 565-567.

Pflug, H.D. and Prössl, K.F., 1991, Palynostratigraphical and paleobotanical studies in the pilot hole of the German continental deep drilling program: results and implications: Scientific Drilling, v. 2, no. 1, p. 13-33.

Pšenička, J., Bek, J., Frýda, J., Žárský, V., Uhlířová, M. and Štorch, P., 2021, Dynamics of Silurian Plants as Response to Climate Changes: Life v. 11, p. 906.

Retallack, G.J., 2015, Silurian vegetation stature and density inferred from fossil soils and plants in Pennsylvania, USA: Journal of the Geological Society, v. 172, no. 6, p. 693-709.

Roberts, S., Tricker, P.M. and Marshall, J.E.A., 1995, Raman spectroscopy of chitinozoans as a maturation indicator: Organic Geochemistry, v. 23, no. 3, p. 223-228.

Romero-Sarmiento, M.F., Riboulleau, A., Vecoli, M. and Versteegh, G.J.M., 2011, Aliphatic and aromatic biomarkers from Gondwanan sediments of Late Ordovician to Early Devonian age: An early terrestrialization approach: Organic Geochemistry, v. 42, no. 6, p. 605-617.

Schito, A., Corrado, S., Trolese, M., Aldega, L., Caricchi, C., Cirilli, S., Grigo, D., Guedes, A., Romano, C., Spina, A. and Valentim, B., 2017, Assessment of thermal evolution of Paleozoic successions of the Holy Cross Mountains (Poland): Marine and Petroleum Geology, v. 80, p. 112-132. https://doi.org/10.1016/j.marpetgeo.2016.11.016

Scott, A.C. and Glasspool, I.J., 2005, Charcoal reflectance as a proxy for the emplacement temperature of pyroclastic flow deposits: Geology, v. 33, no. 7, p. 589-592. https://doi.org/10.1130/G21474.1

Scott, A.C. and Glasspool, I.J., 2007, Observations and experiments on the origin and formation of inertinite group macerals: International Journal of Coal Geology, v. 70, no. 1-3, p. 53-66.

Selosse, M.A., 2002, *Prototaxites*: a 400 MYR old giant fossil, a saprophytic holobasidiomycete, or a lichen?: Mycological Research, v. 106, no. 6, p. 641-644.

Straw, S.H., 1952, The Silurian succession at Cwm Graig Ddu (Breconshire): Geological Journal, v. 1, no. 2, p. 208-219.

Strother, P.K., 1988, New species of *Nematothallus* from the Silurian Bloomsburg Formation of Pennsylvania: Journal of Paleontology, v. 62, p. 967-982.

Suchý, V., Sýkorová, I., Stejskal, M., Šafanda, J., Machovič, V. and Novotná, M., 2002', Dispersed organic matter from Silurian shales of the Barrandian Basin, Czech Republic: optical properties, chemical composition and thermal maturity: International Journal of Coal Geology, v. 53 no. 1, p. 1-25.

Tomescu, A.M., Pratt, L.M., Rothwell, G.W., Strother, P.K. and Nadon, G.C., 2009, Carbon isotopes support the presence of extensive land floras pre-dating the origin of vascular plants: Palaeogeography, Palaeoclimatology, Palaeoecology, v. 283, p. 46-59.

Underdown, R. and Redfern, J., 2008, Petroleum generation and migration in the Ghadames Basin, north Africa: A two-dimensional basin-modeling study: AAPG Bulletin, v. 92, no. 1, p. 53-76.

Wollenweber, J., Schwarzbauer, J., Littke, R., Wilkes, H., Armstroff, A. and Horsfield, B., 2006, Characterisation of non-extractable macromolecular organic matter in Palaeozoic coals: Palaeogeography, Palaeoclimatology, Palaeoecology, v. 240, p. 275-304.

Xianming, X., Wilkins, R.W.T., Dehan, L., Zufa, L. and Jiamu, F., 2000, Investigation of thermal maturity of lower Palaeozoic hydrocarbon source rocks by means of vitrinite-like maceral reflectance-a Tarim Basin case study: Organic Geochemistry, v. 31, no. 10, p. 1041-1052. https://doi.org/10.1016/S0146-6380(00)00061-9

Zalasiewicz, J. and Williams, M., 1999, Graptolite biozonation of the Wenlock Series (Silurian) of the Builth Wells district, central Wales: Geological Magazine, v. 136, no. 3, p. 263-283. https://doi.org/10.1017/S0016756899002599